Thermodynamic Property Measurements for Trifluoromethyl Methyl Ether and Pentafluoroethyl Methyl Ether

Yohei Kayukawa,* Masaya Hasumoto, Takashi Hondo, Yuya Kano, and Koichi Watanabe

School of Science for Open and Environmental Systems, Graduate School of Science and Technology, Keio University, 3-14-1 Hiyoshi, Kohoku-ku, Yokohama 223-8522, Japan

PVT properties are presented for both the gas-phase and liquid-phase, vapor pressures and saturated-liquid densities for hydrofluoroether (HFE) refrigerants, trifluoromethyl methyl ether (CF_3OCH_3) and pentafluoroethyl methyl ether ($C_2F_5OCH_3$), that were obtained with a Burnett apparatus and a vibrating-tube densimeter. A total of 250 liquid densities and 70 gas-phase *PVT* properties for CF_3OCH_3 and 281 liquid densities and 125 gas-phase *PVT* properties for $C_2F_5OCH_3$ were obtained in wide ranges of temperature (240 to 380) K and pressure up to 7 MPa with a rapid density measurement system with a vibrating-tube densimeter. For CF_3OCH_3, 109 gas-phase *PVT* properties were obtained with a Burnett apparatus at the temperatures (300 to 380) K and up to nearly the critical density. On the basis of the present measurements, we have also developed thermodynamic models to complement the experimental data. Equations of state for the liquid phase and truncated virial equations of state are discussed in this paper, as well as a couple of correlations for vapor pressures and saturated-liquid densities.

Introduction

Since energy savings and reduction of carbon dioxide emission are increasingly important concerns, no one would argue about the importance of thermodynamic properties of various working fluids that were used for all types of energy-conversion systems. In particular, there is a pressing need for new environmentally friendly refrigerants with zero ODP (ozone depletion potential) and low GWP (global warming potential), whose data are sufficient to formulate a fully developed equation of state for the purpose of optimum design of such systems and optimum selection of the refrigerant.

Among several alternative candidates of such new refrigerants, HFEs (hydrofluoroethers) are expected to be promising alternative refrigerants due to their short atmospheric lifetimes. Especially, trifluoromethyl methyl ether (CF_3OCH_3) and pentafluoroethyl methyl ether (C_2F_5-OCH_3) have been selected for research in a national project of RITE (the Research Institute of Innovative Technology for the Earth, Japan) to replace dichlorodifluoromethane (CFC12) and 1,2-dichloro-1,1,2,2-tetrafluoroethane (CFC114), respectively.

For these substances, the present authors have teamed up to conduct measurements of fundamental thermodynamic properties including critical parameters[1,2] obtained from a direct observation of a meniscus disappearance with critical opalescence, liquid densities[3,4] with a magnetic-suspension densimeter, and *PVT* properties[5,7] with an isochoric apparatus. Up to now, there were not sufficient data in the gas phase. Also, no liquid density data exist for CF_3OCH_3 below 280 K, due to the limited temperature range of the densimeter. Hence, the range of validity of the thermodynamic models for CF_3OCH_3 and $C_2F_5OCH_3$ by Widiatmo and Watanabe[7,8] is limited to the ranges of these experimental data.

In this study, we have conducted *PVT* property measurements for these substances with a Burnett apparatus and a newly developed vibrating-tube densimeter. The experimental data with the vibrating-tube densimeter apparatus cover wide ranges of temperature down to 240 K and pressure up to 7 MPa, whereas the Burnett measurements cover (300 to 380) K and densities up to $0.75\rho_c$. These experimental data were compared to the thermodynamic models of refs 6 and 7. We also developed original thermodynamic models based on the present measurements.

Experimental Section

Burnett Apparatus. The Burnett method is well-known as effective to obtain densities of a gaseous fluid without any sample-mass weighing. The main operation of this method is to expand the sample gas confined in a sample cell to another expansion vessel evacuated in advance. To repeat such an isothermal expansion and correct a set of isothermal pressure data, each density is calculated from the pressure values and the cell constant, which is the inner volume ratio of the sample cell and the expansion vessel. We have conducted isochoric measurements after each Burnett isothermal expansion in order to obtain *PVT* properties at other temperatures. Details of this apparatus and its calibration are available.[9]

Figure 1 shows a schematic diagram of the present Burnett experimental apparatus. The present apparatus can be divided into three subsystems with their functions, namely, cell system, temperature control and measurement (c/m) system, and pressure c/m system, respectively. The cell system consists of two cells, the sample cell (A) and the expansion vessel (B), which are thick-walled spherical vessels made of stainless steel. These two cells are connected by a constant-volume valve (V1), which is carefully operated in order to prevent any minor pressure inclination. The inner volume ratio at zero pressure is called the cell constant, N_∞, and it was determined precisely using

* To whom correspondence should be addressed. Current address: Fluid Properties Section, Materials Properties and Metrological Statistics Division, National Metrology Institute of Japan, National Institute of Advanced Industrial Science and Technology, AIST Tsukuba Central 3, 1-1-1 Umezono, Tsukuba, Ibaraki 305-8563, Japan. E-mail: yohei@be.mbn.or.jp. Telephone: +81-29-861-6833. Fax: +81-29-850-1464.

10.1021/je025657+ CCC: $25.00
Published on Web 07/11/2003

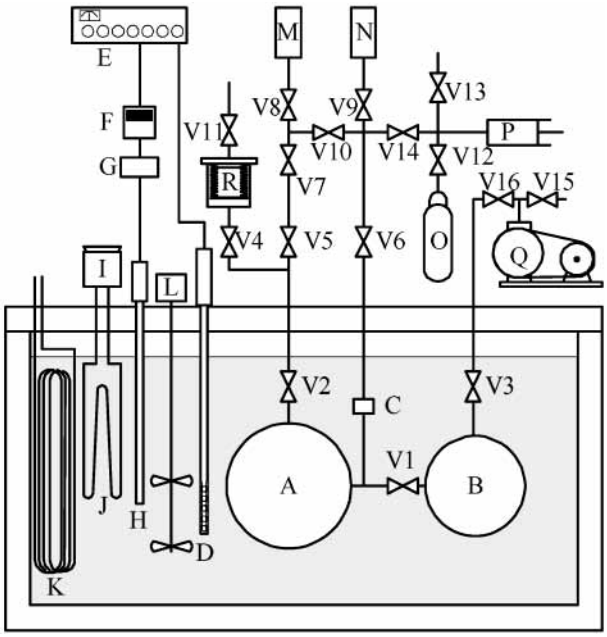

Figure 1. Schematic diagram of the Burnett apparatus at Keio University: A, sample cell; B, expansion vessel; C, differential pressure transducer; D, standard platinum thermometer; E, precision thermometer bridge; F, PID controller; G, thyristor regulator; H, subheater; I, slide transformer; J, main heater; K, water cooler; L, stirrer; M, N, quartz pressure transducer; O, nitrogen gas bomb; P, hand piston; Q, vacuum pump; R, variable volume vessel with metallic bellows; V1, constant volume valve; V2−V13, valves.

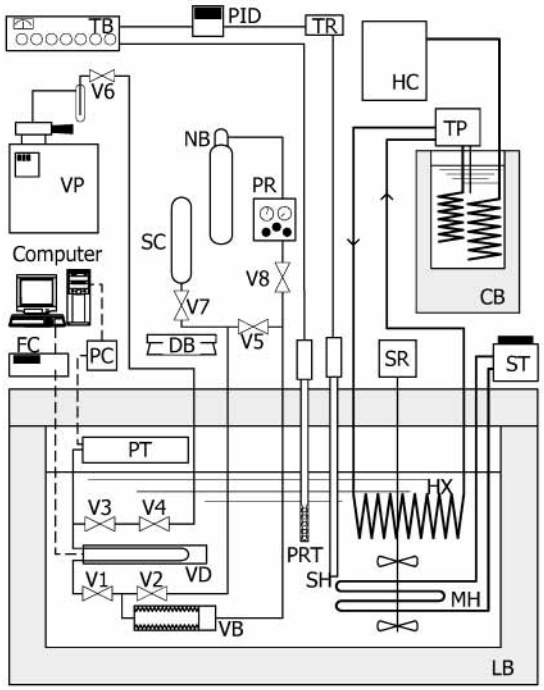

Figure 2. Schematic diagram of the experimental apparatus: VD, densimeter cell; FC, frequency counter; PT, digital pressure gauge; PC, pressure computer; VB, variable volume vessel with metallic bellows; PR, pressure regulator; NB, nitrogen gas bomb; SC, sample supplying cylinder; DB, digital balance; VP, vacuum pump; PRT, standard platinum resistance thermometer; TB, thermometer bridge; LB, liquid bath; PID, PID controller; TR, thyristor regulator; SH, subheater; MH, main heater; ST, slide transformer; SR, stirrer; HX, heat exchanger; TP, temperature regulator pump; CB, cooling bath; HC, handy cooler; V1−7, valves.

gaseous helium with its known density values, being $N_\infty = 1.501\,05 \pm 0.000\,10$. Since it is very difficult to measure the temperature of the sample inside the pressure-proof vessel directly, the sample temperature was measured as the temperature of the bath fluid in which the cell system is immersed. The silicone oil temperature in the vicinity of the sample cell is detected by a standard platinum resistance thermometer (D) and a thermometer bridge (E). A PID controller (F) associated with the thermometer bridge maintains the fluid temperature by controlling the current supplied to the subheater (H) within a fluctuation of ±3 mK.

Concerning the pressure measurements, we have employed an indirect pressure measurement system which consists of a differential pressure indicator, DPI (C), within the thermostated bath. The sample pressure is measured by transmitting it to the nitrogen gas pressure through the DPI made of a thin stainless steel diaphragm which separates the mixture sample from the nitrogen gas.

Experimental uncertainties were estimated, on the basis of the ISO recommendation[10] on the expanded uncertainty with the coverage factor $k = 2$, to be not greater than 7 mK in temperature, 0.8 kPa in pressure, and 0.15 in density. The experimental procedures are described elsewhere.[11,12]

Vibrating-Tube Densimeter. In the present study, liquid densities were obtained by means of our newly developed vibrating-tube densimeter apparatus. The apparatus and measurement procedure are described in detail[13] and will be briefly explained in this subsection.

The principle of vibrating-tube densimetry is simply due to a proportional relation between density, ρ, and the vibrating period squared, τ^2, of the U-shaped tube filled up with the sample fluid. Figure 2 shows a schematic diagram of the present density measurement system. We have employed a commercially available densimeter cell [DMA512, Anton Paar, K. G.], and it is attached beneath a 5.5 kg stainless steel weight which is suspended in a constant-temperature bath fluid (silicone oil) by four coil springs. This structure absorbs shocks and vibration from outside. The sample fluid is charged in the vibrating tube (VD) connected to the pressure gauge (PT) and a variable volume vessel (VB), shut by valves V2 and V4. The sample pressure and volume are regulated by the variable volume vessel with a dynamic metallic bellows by compressing or depressing the bellows by controlling the nitrogen gas pressure outside the bellows appropriately. This set of measurement systems for pressure and density is installed in a precisely temperature-controlled liquid bath (LB). The liquid bath temperature is controlled with the aid of the main heater (MH), a subheater (SH) controlled by a PID controller (PID) which is associated with a precise thermometer bridge (TB), and a standard platinum resistance thermometer (PRT).

The present densimeter was calibrated by measuring the oscillating period under the vacuum and water at different temperature levels; then the sample density is calculated by

$$\rho = A\frac{(1+\mu)x}{1-\mu x} \tag{1}$$

$$x = (\tau^2/{\tau_0}^2) - 1 \tag{2}$$

$$A = (6681.55 - 101.201T^{*0.75} - 29.1168T^{*3})(1 - 0.00164698P^{*}) \tag{3}$$

$$P^{*} = (P/\mathrm{kPa})/7000 \tag{4}$$

$$T^{*} = (T/\mathrm{K})/400 \tag{5}$$

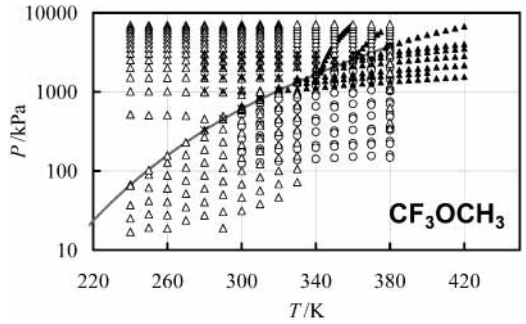

Figure 3. Distribution of the *PVT* data for CF_3OCH_3: ○, this work, Burnett; △, this work, vibrating-tube densimeter; ∗, Morimoto;[3] ▲, Yoneda.[5]

Here, x is a parameter obtained from a vibration period, τ, and that under the vacuum, τ_0. A is a proportionality parameter and is determined by calibration with density-known fluid (water). We have correlated this parameter as a function of temperature and pressure given in eq 3. The parameter μ is a device-dependent constant, being $\mu = 0.0030 \pm 0.0005$. Density measurement uncertainty was confirmed to be within 0.024% and 0.1 kg·m^{-3}. The uncertainty of the present measurements is about 0.022% and 0.26 kPa in pressure and 3 to 7 mK in temperature.

Experimental Results

CF_3OCH_3. A total of 31 vapor pressures and 109 gas-phase *PVT* properties for CF_3OCH_3 were obtained by using the Burnett apparatus along three sets of measurements in the temperature range (300 to 380) K. Seventy *PVT* data in the gas phase and 250 liquid densities were also obtained with the vibrating-tube densimeter apparatus down to 240 K. These experimental data points are illustrated on a $P-T$ diagram in Figure 3, together with those by Morimoto[3] and Yoneda.[5]

We have employed a sample of CF_3OCH_3 with research grade purities, that is, 99.8 mol % for gas-phase *PVT* measurements and 99.98 mol % for vapor pressures and liquid *PVT* measurements. However, there was a small air contaminant found in the sample used for the Burnett measurements. By comparing three sets of vapor pressure data obtained by the Burnett measurements, we found slight differences among them according to the degassing processes conducted in the present measurements. Hence, we have corrected the measured pressure data as follows.

The third series of the vapor pressure measurements with the Burnett apparatus were carefully conducted by introducing the precisely degassed sample into the sample cell little by little to find the saturated-vapor state at respective temperatures. The observed vapor pressures, $P_{s,1}$ [series 1] and $P_{s,2}$ [series 2] were about 12 kPa and 2 kPa lower than those for series 3, $P_{s,3}$, because of air possibly dissolved. By assuming that these vapor pressure differences, $P_{s,1or2} - P_{s,3}$, are eqal to the partial pressure of nitrogen gas, P_{N_2}, the dissolved nitrogen gas densities, ρ_{N_2}, were calculated at respective temperatures with the aid of the formulation given in the IUPAC thermodynamic property tables.[14] Then we have determined the average nitrogen density that might be contained in the sample at the initial stage of measurements to be

$$\rho_{N_2,1} = 0.00470 \pm 0.00017 \text{ mol·m}^{-3} \quad (6)$$

$$\rho_{N_2,2} = 0.00085 \pm 0.00015 \text{ mol·dm}^{-3} \quad (7)$$

Table 1. Experimental Vapor Pressures for CF_3OCH_3 Obtained by the Burnett Apparatus

series 1		series 2		series 3	
T/K	P/kPa	T/K	P/kPa	T/K	P/kPa
300.000	607.7	300.000	607.3	310.000	801.7
305.000	698.7	310.000	800.7	320.000	1038.4
310.000	800.9	320.000	1038.5	330.000	1325.7
315.000	914.3	330.000	1325.6	340.000	1670.2
320.000	1038.1	340.000	1668.5	350.000	2071.7
325.000	1175.7	350.000	2075.0	360.000	2554.9
330.000	1325.7	360.000	2553.8	370.000	3117.1
335.000	1489.7	370.000	3117.3		
340.000	1668.8				
345.000	1863.6				
350.000	2074.9				
355.000	2304.3				
360.000	2553.1				
365.000	2823.3				
370.000	3116.4				
375.000	3435.7				

Therefore, the experimental vapor pressures, $P_{s,exp}$, of the first and second series have been corrected by

$$P_s = P_{s,exp} - P_{IUPAC}(T,\rho_{N_2}) \quad (8)$$

where $P_{IUPAC}(T,\rho_{N_2})$ is calculated from the equation of state for nitrogen by IUPAC.[14] The pressure in the single phase after nth expansions, P_n, is also corrected by

$$P_n = P_{n,exp} - P_{IUPAC}(T,\rho_{N_2}/N^n) \quad (9)$$

since the nitrogen density also decreases with the Burnett expansion. The gas-phase densities by the Burnett measurements were calculated by using thus corrected pressure values.

Concerning the measurements by the vibrating-tube densimeter, a research grade sample with 99.98 mol % furnished by the RITE was used. Table 1 tabulates the corrected vapor pressures for CF_3OCH_3 obtained by the Burnett apparatus. The present experimental *PVT* properties are also summarized in Tables 2 and 3. It should be noted that the same low-density *PVT* data obtained with the vibrating-tube densimeter are marked with a dagger (†) to indicate that they are uncertain data, whereas measurements of saturated liquid densities are marked with an asterisk (*).

$C_2F_5OCH_3$. A total of 281 liquid densities and 125 gas-phase *PVT* properties were obtained for $C_2F_5OCH_3$ as well as a set of the vapor pressures and the saturated-liquid densities at the temperatures (240 to 380) K only by the vibrating-tube densimeter apparatus. These data are tabulated in Table 4. Figure 4 illustrates a distribution of the present data, together with those obtained by Ohta et al.[4] and Widiatmo et al.[6] Concerning the sample purity of $C_2F_5OCH_3$, we have employed a 99.99 mol % purity sample furnished by the RITE.

Discussion

Introductory Remarks. On the basis of the present measurement results, we have developed a set of thermodynamic models so as to correlate and interpolate the experimental data. A pair of correlations for vapor pressures and saturated-liquid densities were formulated as well as truncated virial equations of state and van der Waals type equations of state for gas-phase and liquid-phase *PVT* properties, respectively. These models will be

Table 2. Gas-Phase *PVT* Property Data for CF_3OCH_3 Obtained with the Burnett Apparatus

T/K	*P*/kPa	ρ/kg·m^{-3}	*T*/K	*P*/kPa	ρ/kg·m^{-3}
		Series 1			
380.000	3786.4	439.7	350.000	680.3	25.92
380.000	3686.3	294.2	350.000	469.2	17.27
380.000	3316.9	198.3	350.000	320.6	11.53
380.000	2726.4	131.8	350.000	217.0	7.688
380.000	2092.4	87.73	350.000	146.2	5.127
380.000	1529.5	58.32	340.000	1278.5	58.56
380.000	1084.0	38.82	340.000	929.4	38.95
380.000	752.6	25.86	340.000	655.6	25.94
380.000	515.4	17.23	340.000	453.5	17.28
380.000	350.5	11.51	340.000	310.5	11.54
380.000	236.5	7.671	340.000	210.4	7.694
380.000	158.9	5.114	340.000	141.7	5.126
370.000	3031.6	197.4	330.000	889.0	38.98
370.000	2559.0	132.0	330.000	630.6	25.96
370.000	1990.6	87.72	330.000	437.5	17.29
370.000	1468.6	58.37	330.000	300.2	11.55
370.000	1046.2	38.85	330.000	203.7	7.696
370.000	728.8	25.88	330.000	137.5	5.133
370.000	500.1	17.24	320.000	847.1	38.98
370.000	340.6	11.52	320.000	604.9	25.98
370.000	230.0	7.677	320.000	421.5	17.30
370.000	154.7	5.117	320.000	289.9	11.55
360.000	2385.4	132.0	320.000	197.1	7.701
360.000	1888.4	87.85	320.000	133.1	5.135
360.000	1406.7	58.43	310.000	578.6	25.97
360.000	1007.9	38.88	310.000	405.0	17.30
360.000	704.6	25.90	310.000	279.4	11.56
360.000	484.7	17.25	310.000	190.3	7.705
360.000	330.6	11.52	310.000	128.7	5.137
360.000	223.5	7.683	300.000	550.3	25.89
360.000	150.4	5.122	300.000	388.1	17.29
350.000	1782.8	87.93	300.000	268.7	11.56
350.000	1343.5	58.50	300.000	183.4	7.703
350.000	969.0	38.92	300.000	124.2	5.136
		Series 2			
380.000	3776.4	381.1	350.000	640.8	24.25
380.000	3647.0	276.7	350.000	299.5	10.74
380.000	3233.6	185.9	350.000	202.9	7.174
380.000	2624.1	123.5	340.000	1605.8	82.06
380.000	1994.4	82.12	340.000	1216.9	54.78
380.000	1450.0	54.63	340.000	879.5	36.45
380.000	1023.5	36.37	340.000	425.6	16.13
380.000	708.4	24.22	340.000	195.8	7.136
380.000	483.9	16.12	330.000	841.9	36.48
380.000	327.6	10.73	330.000	594.3	24.27
380.000	220.5	7.140	330.000	410.7	16.13
380.000	147.8	4.751	330.000	280.6	10.75
370.000	2970.3	185.3	330.000	188.9	7.099
370.000	2469.3	123.6	320.000	802.9	36.45
370.000	1901.8	82.19	320.000	570.4	24.28
370.000	1393.4	54.67	320.000	395.7	16.14
370.000	686.1	24.23	320.000	270.9	10.74
370.000	318.3	10.73	320.000	183.4	7.139
370.000	215.6	7.182	310.000	759.9	36.24
360.000	2309.0	123.6	310.000	545.9	24.27
360.000	1807.1	82.26	310.000	380.4	16.14
360.000	1335.8	54.71	310.000	261.0	10.74
360.000	952.6	36.41	310.000	177.1	7.139
360.000	455.0	16.13	300.000	519.4	24.16
360.000	208.1	7.139	300.000	364.7	16.13
350.000	1709.6	82.31	300.000	251.4	10.75
350.000	1277.1	54.75	300.000	170.5	7.128

useful to formulate further multiproperty thermodynamic models such as mBWR or Helmholtz energy equations of state.

Vapor Pressure and Saturated-Liquid Density Correlations. On the basis of the present measurements of the vapor pressures, P_s, and the saturated-liquid densities, ρ', a pair of the correlations given below were developed.

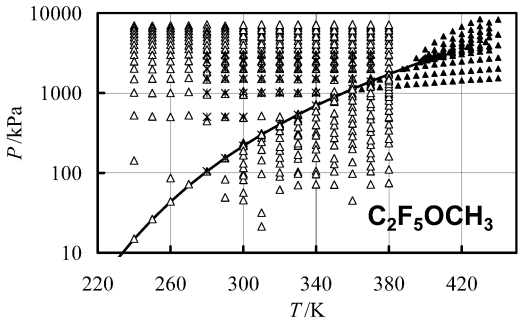

Figure 4. Distribution of the *PVT* data for $C_2F_5OCH_3$: △, this work, vibrating-tube densimeter; ∗, Ohta et al.;[4] ▲, Widiatmo et al.[6]

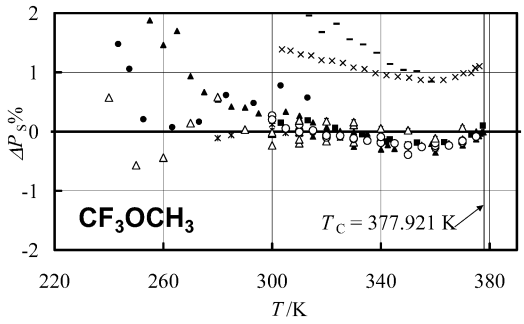

Figure 5. Relative deviation of the vapor pressures of CF_3OCH_3 from eq 10: ○, this work, Burnett; △, this work, vibrating-tube densimeter; —, Kul et al.;[15] ∗, Morimoto;[3] ●, Salvi-Narkhede et al.;[16] ×, Wang et al.;[17] ■, Yasumoto;[18] ▲, Yoneda.[5]

$$\ln \frac{P_s}{P_c} = \frac{T_c}{T}(a_1\tau + a_2\tau^{1.5} + a_3\tau^{2.5} + a_4\tau^5) \qquad (10)$$

$$\frac{\rho'}{\rho_c} = 1 + b_1\tau^{0.33} + b_2\tau^{0.5} + b_3\tau^{1.5} + b_4\tau^{2.5} \qquad (11)$$

$$\tau = 1 - \frac{T}{T_c} \qquad (12)$$

Here, T_c, P_c, and ρ_c denote the critical temperature, pressure, and density, respectively. The numerical constants, a_1 through a_4 and b_1 through b_3, were determined by a least-squares fitting of eqs 10 and 11 to the experimental P_s and ρ' data. These parameters are tabulated in Table 5.

Figures 5−8 illustrate relative deviations of vapor pressures and saturated-liquid densities for CF_3OCH_3 and $C_2F_5OCH_3$ from the present correlations, eqs 10 and 11. From Figures 5 and 6 it was found that eq 10 reproduces most of the present vapor pressure data within ±0.25% at temperatures above 300 K. Since the absolute vapor pressures become very small in the lower temperature range, fluctuations of the present measurements become larger by ±0.6%. The vapor pressures for CF_3OCH_3 reported by Kul et al.[15] and Wang et al.[17] deviate by about +1 to +2%. These differences may be considered to be caused by impurities in the sample used for their measurements. There are also systematic deviations between the present correlation and the vapor pressure data by Widiatmo et al.[6] The present vapor pressures show a similar trend as those by Ohta et al.[4] Concerning the saturated-liquid densities, all the data obtained in the present study are well represented within ±0.1% except a single datum for CF_3OCH_3 at 310 K.

Table 3. Experimental *PVT* Data for CF_3OCH_3 Obtained by the Vibrating-Tube Densimeter Apparatus

T/K	*P*/kPa	ρ/kg·m^{-3}		*T*/K	*P*/kPa	ρ/kg·m^{-3}		*T*/K	*P*/kPa	ρ/kg·m^{-3}		*T*/K	*P*/kPa	ρ/kg·m^{-3}	
Series 1															
300.000	606.0	1086.15	*	320.000	1512.4	1017.85		340.000	3081.7	947.17		360.000	6201.7	897.63	
300.000	658.2	1086.45		320.000	2036.4	1022.49		340.000	3596.1	953.91		360.000	6705.8	905.30	
300.000	1058.4	1088.91		320.000	2520.5	1026.61		340.000	4130.8	960.48		360.000	7100.8	910.94	
300.000	1522.9	1091.63		320.000	3050.4	1030.92		340.000	4614.0	966.04		370.000	3124.3	711.78	*
300.000	2016.1	1094.48		320.000	3595.2	1035.17		340.000	5146.7	971.84		370.000	3147.8	715.08	
300.000	2545.5	1097.41		320.000	4131.4	1039.19		340.000	5642.7	976.95		370.000	3130.2	712.60	
300.000	3063.2	1100.24		320.000	4616.1	1042.69		340.000	6163.1	982.05		370.000	3586.0	754.94	
300.000	3535.6	1102.72		320.000	5136.9	1046.33		340.000	6711.6	987.19		370.000	4068.1	781.44	
300.000	4063.9	1105.45		320.000	5652.1	1049.82		340.000	7112.6	990.78		370.000	4642.5	804.25	
300.000	4569.3	1107.99		320.000	6201.4	1053.41		350.000	2080.3	871.95	*	370.000	5159.1	820.53	
300.000	5140.6	1110.81		320.000	6721.8	1056.72		350.000	2141.2	873.54		370.000	5641.4	833.56	
300.000	5669.7	1113.35		320.000	7175.8	1059.52		350.000	2104.3	872.59		370.000	6176.7	846.09	
300.000	6155.2	1115.66		330.000	1328.7	972.09	*	350.000	2091.1	872.23		370.000	6712.7	857.24	
300.000	6683.2	1118.07		330.000	1458.1	973.66		350.000	2548.5	883.49		370.000	7155.1	865.58	
300.000	7091.7	1119.94		330.000	1414.6	973.15		350.000	3078.0	894.77		380.000	3807.7	489.63	
310.000	802.3	1051.17	*	330.000	1364.9	972.53		350.000	3561.7	903.94		380.000	4003.4	629.00	
310.000	861.7	1051.63		330.000	1329.4	972.09	*	350.000	4061.4	912.50		380.000	4596.7	707.34	
310.000	836.7	1051.44		330.000	2087.0	981.10		350.000	4604.4	920.96		380.000	5159.5	743.66	
310.000	813.1	1051.26		330.000	2555.2	986.24		350.000	5110.9	928.26		380.000	5653.6	766.09	
310.000	1033.6	1052.90		330.000	3114.9	992.08		350.000	5614.7	935.00		380.000	6175.8	785.18	
310.000	1533.9	1056.54		330.000	3553.8	996.38		350.000	6145.6	941.66		380.000	6672.5	800.32	
310.000	2046.2	1060.13		330.000	4105.6	1001.58		350.000	6708.6	948.27		380.000	7138.9	812.70	
310.000	2539.9	1063.48		330.000	4643.4	1006.39		350.000	7180.7	953.51		380.000	3791.1	430.78	
310.000	3099.5	1067.15		330.000	5117.0	1010.47		360.000	2557.0	805.64	*	380.000	3672.6	287.87	
310.000	3564.5	1070.10		330.000	5639.1	1014.76		360.000	2674.0	811.00		380.000	3383.7	207.93	
310.000	4131.5	1073.59		330.000	6168.6	1018.96		360.000	2595.3	807.47		380.000	2913.0	148.72	
310.000	5149.7	1079.59		330.000	6739.6	1023.31		360.000	2566.6	806.04		380.000	2282.2	99.68	
310.000	5630.8	1082.31		330.000	7155.4	1026.38		360.000	3046.9	825.94		380.000	1736.8	68.74	
310.000	6210.4	1085.50		340.000	1672.6	925.57	*	360.000	3567.7	842.69		380.000	1190.9	43.52	
310.000	7191.1	1090.69		340.000	1776.3	927.36		360.000	4099.1	856.85		380.000	1069.0	38.43	
320.000	1040.9	1013.47	*	340.000	1704.5	926.14		360.000	4614.4	868.64		380.000	637.2	21.72	
320.000	1117.7	1014.21		340.000	1691.6	925.88		360.000	5110.0	878.67		380.000	411.6	13.64	†
320.000	1081.4	1013.85		340.000	2059.3	932.03		360.000	5611.7	887.84		380.000	345.8	11.40	†
320.000	1046.3	1013.52		340.000	2582.2	940.10		360.000	6215.7	897.87					
Series 2															
240.000	36.9	1.87	†	250.000	2020.1	1240.28		270.000	6036.1	1199.08		280.000	454.4	1150.61	
240.000	25.1	1.25	†	250.000	1508.8	1238.91		270.000	5542.1	1197.53		290.000	449.6	1119.31	*
240.000	17.0	0.84	†	250.000	1008.8	1237.55		270.000	5047.2	1195.96		290.000	338.9	15.78	†
240.000	67.4	1261.55	*	250.000	505.1	1236.18		270.000	4513.3	1194.24		290.000	232.8	10.52	†
240.000	6981.1	1277.36		250.000	102.6	1235.07	*	270.000	4038.2	1192.68		290.000	159.4	7.09	†
240.000	6511.7	1276.35		260.000	127.7	6.40	†	270.000	3484.3	1190.86		290.000	109.0	4.83	†
240.000	6024.7	1275.29		260.000	87.8	4.40	†	270.000	3017.0	1189.29		290.000	74.2	3.26	†
240.000	5511.8	1274.16		260.000	59.9	3.03	†	270.000	2500.7	1187.53		290.000	50.3	2.25	†
240.000	5038.9	1273.12		260.000	40.7	2.15	†	270.000	1999.2	1185.81		290.000	30.4	1.28	†
240.000	4515.5	1271.95		260.000	27.6	1.53	†	270.000	1515.4	1184.10		290.000	18.9	0.76	†
240.000	4031.0	1270.86		260.000	18.7	1.11	†	270.000	1001.8	1182.27		290.000	6981.5	1148.28	
240.000	3529.6	1269.72		260.000	6987.4	1227.99		270.000	500.8	1180.45		290.000	6496.3	1146.42	
240.000	3024.1	1268.56		260.000	6546.9	1226.81		270.000	229.7	1179.44	*	290.000	6046.4	1144.61	
240.000	2517.3	1267.38		260.000	6040.8	1225.42		280.000	327.4	1150.07	*	290.000	5546.1	1142.55	
240.000	2014.7	1266.21		260.000	5512.3	1223.96		280.000	269.0	12.52	†	290.000	4999.6	1140.25	
240.000	1516.2	1265.03		260.000	5039.1	1222.63		280.000	186.4	8.53	†	290.000	4505.0	1138.14	
240.000	1011.0	1263.83		260.000	4522.0	1221.16		280.000	128.3	5.75	†	290.000	4029.3	1136.09	
240.000	517.1	1262.64		260.000	4018.0	1219.71		280.000	87.6	3.89	†	290.000	3492.2	1133.73	
240.000	65.5	1261.54	*	260.000	3527.2	1218.29		280.000	59.6	2.61	†	290.000	2989.9	1131.43	
250.000	89.4	4.33	†	260.000	3012.1	1216.77		280.000	40.5	1.79	†	290.000	2466.6	1129.04	
250.000	61.2	2.94	†	260.000	2515.8	1215.30		280.000	27.5	1.21	†	290.000	1999.9	1126.86	
250.000	41.7	1.98	†	260.000	2004.5	1213.76		280.000	7008.7	1175.70		290.000	1475.8	1124.36	
250.000	28.3	1.34	†	260.000	1499.4	1212.21		280.000	6516.6	1173.99		290.000	976.7	1121.93	
250.000	19.2	0.91	†	260.000	1009.3	1210.70		280.000	5977.4	1172.09		290.000	979.3	1121.87	
250.000	6975.1	1252.79		260.000	507.8	1209.12		280.000	5533.2	1170.51		290.000	493.5	1119.50	
250.000	6529.6	1251.71		260.000	156.0	1208.02	*	280.000	4942.1	1168.36		300.000	605.9	1086.56	*
250.000	6026.5	1250.48		270.000	160.6	7.63	†	280.000	4483.8	1166.68		300.000	589.3	28.11	
250.000	5550.6	1249.31		270.000	110.6	5.15	†	280.000	4037.2	1164.99		300.000	439.5	19.94	†
250.000	5042.6	1248.05		270.000	75.7	3.49	†	280.000	3522.2	1163.04		300.000	306.3	13.34	†
250.000	4537.2	1246.78		270.000	51.5	2.35	†	280.000	3011.5	1161.06		300.000	214.0	9.08	†
250.000	4030.5	1245.49		270.000	35.0	1.60	†	280.000	2510.8	1159.10		300.000	146.6	6.12	†
250.000	3530.8	1244.22		270.000	23.7	1.10	†	280.000	1992.9	1157.02		300.000	100.1	4.12	†
250.000	3037.0	1242.95		270.000	6973.6	1201.96		280.000	1507.7	1155.03		300.000	68.0	2.77	†
250.000	2517.2	1241.59		270.000	6529.6	1200.61		280.000	985.2	1152.87					

Table 3 (Continued)

T/K	*P*/kPa	ρ/kg·m^{-3}		*T*/K	*P*/kPa	ρ/kg·m^{-3}		*T*/K	*P*/kPa	ρ/kg·m^{-3}		*T*/K	*P*/kPa	ρ/kg·m^{-3}	
Series 2 (Continued)															
300.000	46.2	1.89	†	310.000	742.6	35.17		310.000	2498.6	1063.70		320.000	5039.6	1046.35	
300.000	31.3	1.25	†	310.000	528.4	23.40		310.000	2000.5	1060.31		320.000	4518.5	1042.67	
300.000	604.7	1086.47	*	310.000	372.5	15.80	†	310.000	1512.4	1056.88		320.000	4030.7	1039.11	
300.000	6960.3	1119.71		310.000	258.9	10.69	†	310.000	1006.3	1053.19		320.000	3512.7	1035.21	
300.000	6499.0	1117.65		310.000	178.2	7.22	†	320.000	1037.4	1014.09	*	320.000	3012.2	1031.29	
300.000	6023.0	1115.44		310.000	121.9	4.87	†	320.000	968.5	46.37		320.000	2529.1	1027.35	
300.000	5517.0	1113.05		310.000	83.1	3.29	†	320.000	634.7	27.54		320.000	2029.1	1023.10	
300.000	5014.6	1110.58		310.000	56.5	2.22	†	320.000	449.1	18.62	†	320.000	1515.2	1018.55	
300.000	4499.8	1108.05		310.000	38.3	1.49	†	320.000	312.9	12.57	†	330.000	1359.2	973.36	*
300.000	4015.2	1105.57		310.000	799.7	1051.64	*	320.000	215.4	8.49	†	330.000	936.5	41.69	
300.000	3486.7	1102.83		310.000	6998.0	1090.22		320.000	147.5	5.74	†	330.000	674.2	28.13	
300.000	3023.5	1100.35		310.000	6538.6	1087.83		320.000	100.6	3.89	†	330.000	475.1	19.02	†
300.000	2526.4	1097.64		310.000	6021.1	1085.02		320.000	68.4	2.64	†	330.000	330.5	12.87	†
300.000	1998.6	1094.68		310.000	5542.0	1082.34		320.000	46.4	1.77	†	330.000	227.6	8.70	†
300.000	1466.6	1091.63		310.000	5049.8	1079.54		320.000	6877.8	1058.42		330.000	155.7	5.88	†
300.000	913.6	1088.34		310.000	4531.7	1076.50		320.000	6522.4	1056.19		330.000	106.1	3.97	†
300.000	617.0	1086.54		310.000	4017.7	1073.40		320.000	6055.9	1053.18		330.000	72.1	2.70	†
310.000	800.7	1054.68	*	310.000	3517.0	1070.31		320.000	5518.0	1049.62		330.000	1324.8	973.37	*
310.000	799.2	1054.67	*	310.000	3027.3	1067.18									

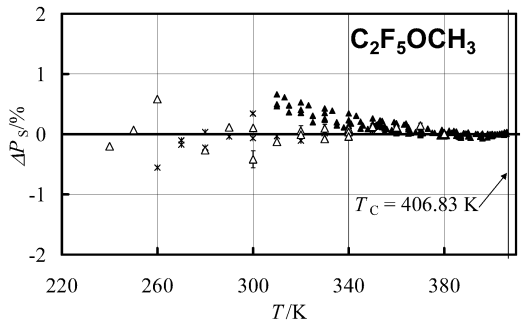

Figure 6. Relative deviation of the vapor pressures of $C_2F_5OCH_3$ from eq 10: △, this work, vibrating-tube densimeter; ∗, Ohta et al.;[4] ▲, Widiatmo et al.[6]

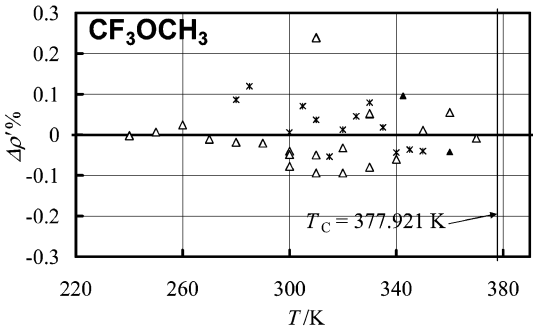

Figure 7. Relative deviation of the saturated-liquid densities of CF_3OCH_3 from eq 11: △, this work, vibrating-tube densimeter; ∗, Morimoto;[3] ▲, Yoneda.[5]

Virial Equations of State. To represent the gas-phase thermodynamic properties for HFEs measured in the present study, truncated virial equations of state were developed. The compressibility factor, *Z*, is expressed by

$$Z = 1 + B(T)\rho + C(T)\rho^2 + D(T)\rho^3 \qquad (13)$$

B(*T*), *C*(*T*), and *D*(*T*) are the second, third, and fourth virial coefficients, respectively. We have used following functions of reduced temperature, $T_r = T/T_c$, to express these virial coefficients.

$$B(T)\rho_c = b_1 + b_2 T_r^{-1} + b_3 \exp(T_r^{-1}) \qquad (14)$$

$$C(T)\rho_c^2 = c_1 + c_2 T_r^{-8} + c_3 T_r^{-13} \qquad (15)$$

$$D(T)\rho_c^3 = d_1 T_r^{-3} \qquad (16)$$

The functional form of the second virial coefficient correlation, eq 14, was originally proposed by Zhang.[9] Parameters b_1 through d_1 have been determined by the least-squares fitting of eq 13 to the present experimental results of gas-phase *PVT* properties for CF_3OCH_3 and $C_2F_5OCH_3$. Table 6 summarizes thus optimized numerical constants. The critical temperature and density values are tabulated in Table 5.

Figures 9 and 10 illustrate percent deviations of the present *PVT* property data from the virial equation of state, eq 13. Isochoric data obtained by Yoneda[5] for CF_3OCH_3 and Widiatmo et al.[6] for $C_2F_5OCH_3$ are also included in these deviation diagrams. From Figure 9, it is found that all the

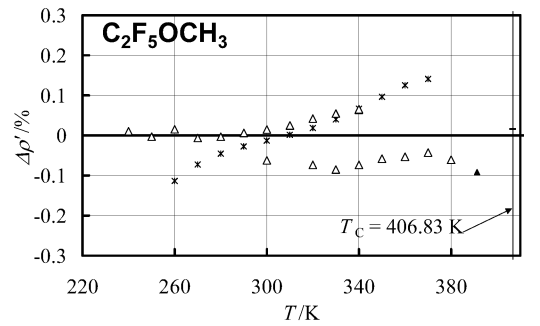

Figure 8. Relative deviation of the saturated-liquid densities of $C_2F_5OCH_3$ from eq 11: △, this work, vibrating-tube densimeter; ∗, Ohta et al.;[4] ▲, Widiatmo et al.[6]

present data for CF_3OCH_3 obtained with the Burnett apparatus are well represented by the EoS within ±0.23%. Most of the present data are excellently reproduced only within ±0.1%. The data obtained with the vibrating-tube densimeter apparatus, on the other hand, show somewhat larger scatter than those by the Burnett apparatus, especially at lower densities. At densities above 10 kg·m^{-3}, however, fluctuations are not greater than ±0.4%. In the present study, we have judged the effective lower limit of density measurement by the vibrating-tube densimeter to be down to 20 kg·m^{-3}. The isochoric measurements by Yoneda[5] are confirmed to be well represented by eq 13 within ±0.46%, except two data points at the density 447 kg·m^{-3} in the very vicinity of the critical point[1] (ρ_c = 465 kg·m^{-3}).

Table 4. Experimental *PVT* Data for $C_2F_5OCH_3$ Obtained by the Vibrating-Tube Densimeter Apparatus

T/K	*P*/kPa	ρ/kg·m^{-3}		*T*/K	*P*/kPa	ρ/kg·m^{-3}		*T*/K	*P*/kPa	ρ/kg·m^{-3}		*T*/K	*P*/kPa	ρ/kg·m^{-3}	
Series 1															
300.000	216.7	1260.39	*	320.000	2051.9	1207.02		340.000	4072.4	1154.47		360.000	7245.1	1113.38	
300.000	238.5	1260.72		320.000	3053.1	1213.09		340.000	5093.0	1162.13		370.000	1395.3	991.98	*
300.000	225.7	1260.66		320.000	4120.2	1219.20		340.000	6115.2	1169.40		370.000	1431.7	992.85	
300.000	1060.7	1264.75		320.000	5085.4	1224.49		340.000	7160.8	1176.36		370.000	1404.3	992.20	
300.000	2031.9	1269.32		320.000	6206.6	1230.35		350.000	889.2	1084.74	*	370.000	2031.8	1006.03	
300.000	3055.9	1273.93		320.000	7182.7	1235.21		350.000	902.4	1084.92		370.000	3042.0	1024.99	
300.000	4031.8	1278.16		330.000	535.9	1161.46	*	350.000	933.0	1085.29		370.000	4077.7	1041.14	
300.000	5197.0	1282.99		330.000	547.4	1161.55		350.000	1049.9	1086.78		370.000	5127.4	1055.31	
300.000	6173.2	1286.91		330.000	1004.0	1165.27		350.000	2056.5	1098.92		370.000	6112.9	1067.19	
300.000	7126.4	1290.50		330.000	1999.0	1172.99		350.000	3061.7	1109.59		370.000	7213.4	1079.13	
310.000	312.6	1229.37		330.000	2033.5	1173.24		350.000	4100.2	1119.85		380.000	1716.3	934.86	*
310.000	300.3	1229.27		330.000	3040.4	1180.50		350.000	5116.8	1128.93		380.000	1807.8	938.21	
310.000	1029.3	1233.39		330.000	4054.0	1187.37		350.000	6125.5	1137.30		380.000	1785.0	937.35	
310.000	2065.7	1238.99		330.000	5095.2	1194.02		350.000	7196.9	1145.60		380.000	1763.3	936.59	
310.000	3131.6	1244.48		330.000	6121.5	1200.18		360.000	1120.4	1040.97	*	380.000	1744.3	935.88	
310.000	4126.7	1249.38		330.000	7184.0	1206.23		360.000	1139.7	1041.29		380.000	2057.3	946.70	
310.000	5145.5	1254.18		340.000	695.6	1124.55	*	360.000	1228.0	1042.77		380.000	3036.6	973.66	
310.000	6158.3	1258.81		340.000	722.8	1124.82		360.000	2053.3	1055.56		380.000	4035.7	994.89	
310.000	7224.0	1263.45		340.000	707.0	1124.67		360.000	3048.1	1069.38		380.000	5093.2	1013.21	
320.000	405.4	1196.29	*	340.000	1053.7	1128.14		360.000	4078.7	1081.81		380.000	6103.7	1028.48	
320.000	413.8	1196.33		340.000	1999.2	1137.11		360.000	5093.9	1092.92		380.000	7127.1	1041.96	
320.000	1053.0	1200.63		340.000	3017.0	1145.96		360.000	6147.8	1103.45					
Series 2															
240.000	142.7	1425.44		260.000	44.1	1374.20	*	290.000	153.7	1291.09	*	320.000	2002.9	1208.23	
240.000	6991.3	1440.14		270.000	72.6	1347.19	*	300.000	7023.9	1291.24		320.000	1521.8	1205.15	
240.000	6522.4	1439.20		270.000	6977.7	1367.99		300.000	6524.7	1289.29		320.000	1023.1	1201.87	
240.000	6031.3	1438.18		270.000	6512.4	1366.76		300.000	5997.8	1287.18		320.000	506.3	1198.36	
240.000	5507.4	1437.10		270.000	6030.4	1365.42		300.000	5491.3	1285.12		320.000	405.1	1197.68	*
240.000	5006.8	1436.06		270.000	5514.7	1363.95		300.000	4978.0	1283.00		320.000	383.0	24.92	
240.000	4516.7	1435.03		270.000	5023.1	1362.54		300.000	4522.9	1281.10		320.000	191.5	11.50	†
240.000	4022.9	1433.98		270.000	4491.8	1360.99		300.000	4031.0	1279.00		320.000	132.0	7.77	†
240.000	3526.2	1432.91		270.000	3956.7	1359.43		300.000	3514.0	1276.75		320.000	90.4	5.23	†
240.000	3020.1	1431.83		270.000	3549.7	1358.22		300.000	2993.2	1274.45		320.000	61.7	3.58	†
240.000	2495.8	1430.67		270.000	3044.2	1356.70		300.000	2496.4	1272.22		330.000	472.9	30.25	
240.000	2020.0	1429.64		270.000	2522.2	1355.11		300.000	2019.0	1270.02		330.000	315.2	18.98	†
240.000	1498.9	1428.49		270.000	2026.1	1353.57		300.000	1531.0	1267.74		330.000	219.7	12.83	
240.000	1016.6	1427.42		270.000	1545.3	1352.07		300.000	953.1	1264.98		330.000	151.6	8.67	†
240.000	525.8	1426.30		270.000	1033.1	1350.45		300.000	491.2	1262.72		330.000	103.9	5.88	†
240.000	15.1	1425.22	*	270.000	526.2	1348.82		300.000	217.8	1261.37	*	330.000	70.8	3.97	†
250.000	6941.8	1416.34		280.000	104.7	1319.62	*	300.000	98.2	6.15	†	330.000	7006.4	1207.37	
250.000	6505.2	1415.37		280.000	7194.3	1343.64		300.000	45.7	2.84	†	330.000	6544.9	1204.73	
250.000	5982.1	1414.17		280.000	6466.8	1341.37		310.000	276.7	17.86	†	330.000	6004.2	1201.54	
250.000	5520.4	1413.12		280.000	5847.1	1339.41		310.000	31.7	1.86	†	330.000	5526.8	1198.64	
250.000	5017.1	1411.96		280.000	5492.2	1338.26		310.000	21.5	1.25	†	330.000	5044.3	1195.65	
250.000	4527.8	1410.82		280.000	4981.9	1336.62		310.000	7010.8	1264.09		330.000	4522.8	1192.32	
250.000	4031.6	1409.66		280.000	4513.2	1335.09		310.000	6533.8	1261.96		330.000	4007.5	1188.95	
250.000	3493.4	1408.39		280.000	3963.9	1333.26		310.000	6031.8	1259.71		330.000	3527.6	1185.73	
250.000	3006.1	1407.22		280.000	3497.7	1331.69		310.000	5514.9	1257.34		330.000	3014.1	1182.15	
250.000	2484.2	1405.96		280.000	2951.9	1329.83		310.000	5034.7	1255.08		330.000	2499.3	1178.46	
250.000	1981.4	1404.73		280.000	2459.7	1328.12		310.000	4507.3	1252.57		330.000	2009.1	1174.81	
250.000	1512.6	1403.57		280.000	1861.1	1326.03		310.000	3972.8	1249.95		330.000	1493.2	1170.86	
250.000	999.4	1402.28		280.000	1474.3	1324.63		310.000	3532.8	1247.78		330.000	1009.1	1167.02	
250.000	508.4	1401.06		280.000	957.2	1322.76		310.000	3064.4	1245.40		330.000	535.0	1163.08	*
250.000	26.5	1399.85	*	280.000	445.3	1320.87		310.000	2524.9	1242.60		340.000	695.2	1126.10	*
260.000	86.5	1374.31		290.000	83.3	1290.78		310.000	2033.1	1239.99		340.000	7001.9	1177.33	
260.000	6976.1	1392.71		290.000	6967.8	1317.32		310.000	1513.8	1237.16		340.000	6527.2	1174.25	
260.000	6497.8	1391.53		290.000	6484.8	1315.61		310.000	1007.8	1234.36		340.000	6030.7	1170.83	
260.000	6029.6	1390.36		290.000	6024.9	1313.97		310.000	517.0	1231.54		340.000	5487.3	1166.99	
260.000	5494.8	1389.00		290.000	5527.4	1312.20		310.000	300.0	1230.28	*	340.000	5046.6	1163.80	
260.000	5008.9	1387.75		290.000	4985.1	1310.22		320.000	6965.6	1236.06		340.000	4525.8	1159.90	
260.000	4516.6	1386.48		290.000	4525.3	1308.51		320.000	6495.8	1233.69		340.000	3993.9	1155.78	
260.000	4009.1	1385.14		290.000	4006.3	1306.56		320.000	5992.8	1231.09		340.000	3529.7	1152.07	
260.000	3509.7	1383.80		290.000	3491.2	1304.61		320.000	5551.9	1228.77		340.000	3002.4	1147.70	
260.000	3006.5	1382.45		290.000	2991.9	1302.67		320.000	5018.6	1225.90		340.000	2516.0	1143.49	
260.000	2509.7	1381.11		290.000	2520.4	1300.82		320.000	4543.1	1223.30		340.000	2020.3	1139.04	
260.000	2001.0	1379.71		290.000	2011.5	1298.79		320.000	4012.9	1220.32		340.000	1524.7	1134.41	
260.000	1516.5	1378.35		290.000	1520.9	1296.80		320.000	3517.5	1217.45		340.000	1026.7	1129.54	
260.000	1002.7	1376.90		290.000	981.6	1294.58		320.000	3022.6	1214.49		340.000	694.7	1126.12	*
260.000	500.8	1375.48		290.000	504.8	1292.57		320.000	2517.3	1211.43		340.000	597.2	38.04	

Table 4 (Continued)

T/K	P/kPa	ρ/kg·m^{-3}		T/K	P/kPa	ρ/kg·m^{-3}		T/K	P/kPa	ρ/kg·m^{-3}		T/K	P/kPa	ρ/kg·m^{-3}	
Series 2 (Continued)															
340.000	323.2	18.70	†	350.000	888.1	1086.06	*	370.000	1277.5	87.49		370.000	1391.7	992.32	*
340.000	224.8	12.57	†	360.000	1119.1	1042.21	*	370.000	1224.5	81.87		380.000	7011.9	1041.19	
340.000	154.8	8.59	†	360.000	6997.3	1113.07		370.000	920.6	55.26		380.000	6514.1	1034.76	
340.000	106.0	5.76	†	360.000	6519.9	1108.71		370.000	666.8	37.39		380.000	6032.6	1028.11	
340.000	72.2	3.93	†	360.000	5980.2	1103.61		370.000	471.8	25.21		380.000	5510.3	1020.45	
350.000	777.4	50.08		360.000	5527.2	1099.14		370.000	328.5	16.95	†	380.000	4998.2	1012.37	
350.000	560.7	33.51		360.000	5021.2	1093.94		370.000	226.2	11.41	†	380.000	4514.5	1004.14	
350.000	395.0	22.40		360.000	4467.5	1087.96		370.000	154.8	7.64	†	380.000	4004.9	994.70	
350.000	275.0	15.14	†	360.000	4021.5	1082.91		370.000	105.5	5.15	†	380.000	3496.2	984.34	
350.000	129.8	6.86	†	360.000	3506.1	1076.76		370.000	71.6	3.44	†	380.000	2986.2	972.71	
350.000	6996.6	1145.86		360.000	2984.8	1070.14		370.000	1393.3	992.42	*	380.000	2481.3	959.56	
350.000	6531.4	1142.27		360.000	2463.0	1063.09		370.000	6886.1	1076.82		380.000	1715.1	935.87	*
350.000	5973.9	1137.80		360.000	2003.3	1056.42		370.000	6526.3	1072.95		380.000	1499.7	103.34	
350.000	5469.1	1133.62		360.000	1529.8	1049.05		370.000	5982.5	1066.79		380.000	1486.5	101.79	
350.000	4979.5	1129.41		360.000	1118.8	1042.15	*	370.000	5527.5	1061.36		380.000	1299.2	82.86	
350.000	4481.5	1124.97		360.000	990.4	65.14		370.000	5031.9	1055.14		380.000	969.2	56.06	
350.000	4005.1	1120.60		360.000	915.4	58.53		370.000	4515.8	1048.28		380.000	697.5	37.81	
350.000	3474.5	1115.43		360.000	670.7	39.54		370.000	4012.1	1041.13		380.000	492.2	25.55	
350.000	3024.3	1110.87		360.000	477.9	26.77		370.000	3496.9	1033.20		380.000	342.4	17.25	†
350.000	2517.3	1105.50		360.000	334.5	18.07	†	370.000	3015.7	1025.26		380.000	235.9	11.67	†
350.000	2013.5	1099.88		360.000	231.4	12.20	†	370.000	2519.7	1016.39		380.000	161.5	7.87	†
350.000	1470.3	1093.45		360.000	98.2	5.11	†	370.000	1998.7	1006.05		380.000	110.1	5.30	†
350.000	1008.2	1087.64		360.000	45.3	2.31	†	370.000	1520.0	995.40		380.000	74.8	3.57	†
Series 3 (Continued)															
300.000	217.0	1261.41	*	320.000	336.5	21.52		350.000	455.2	26.40		370.000	370.0	19.53	†
300.000	218.2	15.51	*†	320.000	384.9	25.11		350.000	319.9	17.93	†	370.000	256.7	13.19	†
300.000	165.9	10.97	†	320.000	389.1	25.46		350.000	222.0	12.14	†	370.000	176.6	8.92	†
300.000	116.1	7.55	†	330.000	98.4	5.48	†	350.000	152.8	8.19	†	370.000	120.9	6.04	†
300.000	82.0	5.31	†	330.000	169.4	9.72	†	350.000	104.7	5.60	†	380.000	1712.5	133.96	*
300.000	56.7	3.73	†	330.000	235.2	13.71	†	350.000	71.4	3.80	†	380.000	1530.9	107.11	
300.000	188.8	12.58	†	330.000	307.4	18.42	†	360.000	1112.9	77.81	*	380.000	268.9	13.32	†
300.000	131.7	8.60	†	330.000	295.3	17.66	†	360.000	807.9	49.64		380.000	408.5	20.83	
300.000	93.3	6.05	†	330.000	375.8	23.12		360.000	586.1	33.71		380.000	502.4	26.12	
310.000	301.1	23.61	*	330.000	444.8	28.23		360.000	415.3	22.84		380.000	602.7	31.98	
310.000	97.3	5.82	†	340.000	695.2	47.90	*	360.000	289.8	15.49	†	380.000	703.9	38.16	
310.000	144.4	8.89	†	340.000	97.1	5.22	†	360.000	200.1	10.49	†	380.000	804.6	44.65	
310.000	195.7	12.34	†	340.000	198.1	11.09	†	360.000	137.2	7.10	†	380.000	899.8	51.10	
310.000	245.2	15.73	†	340.000	295.9	17.05	†	370.000	1391.5	101.33	*	380.000	1019.1	59.71	
320.000	405.4	29.81	*	340.000	396.6	23.61		370.000	1278.1	88.01		380.000	1101.8	66.08	
320.000	101.6	5.98	†	340.000	495.8	30.46		370.000	1205.2	80.41		380.000	1212.9	75.17	
320.000	155.5	9.32	†	340.000	596.0	38.08		370.000	1005.3	62.34		380.000	1295.3	82.53	
320.000	213.2	12.95	†	350.000	888.5	61.38	*	370.000	737.9	42.35		380.000	1417.2	94.38	
320.000	276.1	17.25	†	350.000	799.2	52.12		370.000	527.2	28.67		380.000	1486.8	101.80	

Table 5. Numerical Constants for Eqs 10 and 11

	CF_3OCH_3	$C_2F_5OCH_3$
T_c/K	377.921	406.83
P_c/kPa	3635	2887
ρ_c/kg·m^{-3}	465	509
a_1	−7.275 209	−7.736 584
a_2	1.076 442	1.583 781
a_3	−1.039 023	−2.153 185
a_4	−8.245 100	−9.491 071
b_1	1.643 119	1.816 187
b_2	−0.220 995	−0.515 149
b_3	−0.372 466	0.023 164
b_4	0.441 701	

Table 6. Numerical Constants for Eqs 13−16

	CF_3OCH_3	$C_2F_5OCH_3$
b_1	2.319 988	2.288 861
b_2	3.196 975	3.582 477
b_3	−2.580 863	−2.690 422
c_1	0.583 774	0.486 753
c_2	0.545 129	0.476 663
c_3	−0.125 585	−0.150 784
d_1	−0.257 111	0.031 388

The compared results were similar in the case of $C_2F_5OCH_3$ shown in Figure 10. At the effective density range of the measurements by the vibrating-tube densimeter (ρ > 20 kg·m^{-3}), all the present data are well reproduced by eq 13 within ±0.35%. There are systematic deviations found for the isochoric data by Widiatmo et al.[6] at higher densities, since the present measurements that were used as input data for the virial EoS have lower densities than 100 kg·m^{-3}.

To confirm the soundness of the virial EoS developed in this study, we have examined the temperature dependence of the second virial coefficient. Figures 11 and 12 illustrate the calculated curves of the second virial coefficients by eq 14 together with experimentally determined values by the present study. We can observe thermodynamically sound behavior of the second virial coefficients for both CF_3OCH_3 and $C_2F_5OCH_3$. The experimental second virial coefficients agree well with the calculated curves within a few percent, but they slightly deviate at lower temperatures for CF_3OCH_3. At lower temperatures, the relative uncertainty of the gas density increases due to the lower absolute value of the saturated-vapor density. In such a temperature range, the evaluated value of the second virial coefficient strongly depends on a fitting procedure such as a weighting factor.

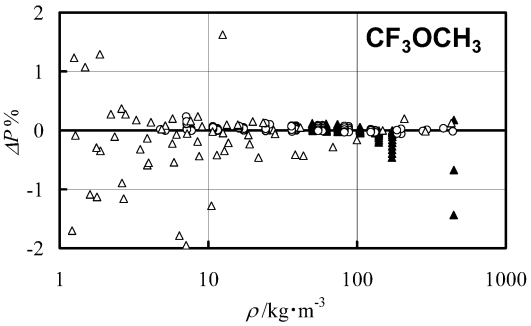

Figure 9. Relative pressure deviation of the gas-phase *PVT* properties of CF_3OCH_3 from eq 13: ○, this work, Burnett; △, this work, vibrating-tube densimeter; ▲, Yoneda.[5]

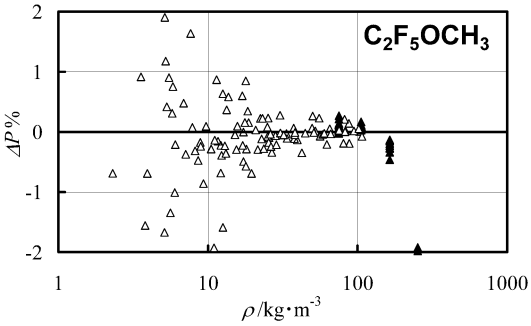

Figure 10. Relative pressure deviation of the gas-phase *PVT* properties of $C_2F_5OCH_3$ from eq 13: △, this work, vibrating-tube densimeter; ▲, Widiatmo et al.[6]

It seems hard to extend a similar discussion on the third virial coefficients, since they are difficult to obtain precisely from the experimental *PVT* property results. However, we have confirmed physically sound behavior of the calculated curves of the third virial coefficients. Some derived properties, including heat capacities and speeds of sounds, were also calculated from the present virial EoS and were found to behave thermodynamically rationally.

Equations of State for the Liquid Phase. To represent the thermodynamic properties in the liquid phase of CF_3OCH_3 and $C_2F_5OCH_3$, we have developed empirical equations of state. The original basic function of the EoS was proposed by Sato[19] to represent the thermodynamic properties of water, as a modified form of the van der Waals equation of state. We have employed this basic function to represent the liquid-phase thermodynamic properties for CF_3OCH_3 and $C_2F_5OCH_3$. The functional form of the EoS is given by

$$\rho_r = \frac{(P_r + A(T_r))^{C(T_r)}}{D(T_r)} \tag{17}$$

$$A(T) = \sum_{k=0}^{2} a_i T_r^{\,k} \tag{18}$$

$$C(T) = \sum_{k=0}^{2} c_i T_r^{\,k} \tag{19}$$

$$D(T) = \sum_{k=0}^{3} d_i T_r^{\,k} \tag{20}$$

In the present study, the numerical constants a_0 through d_3 were determined by the nonlinear regression of the EoS

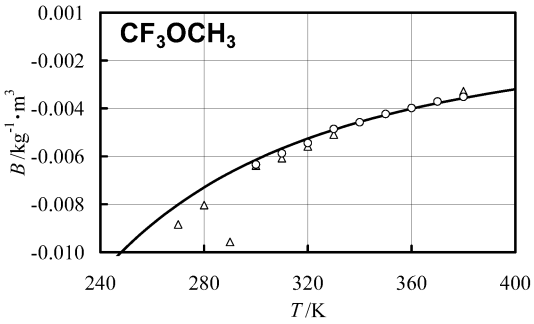

Figure 11. Temperature dependence of the second virial coefficient for CF_3OCH_3: ○, experimental values by this work, Burnett; △, experimental values by this work, vibrating-tube densimeter; - - -, calculated curve by eq 14.

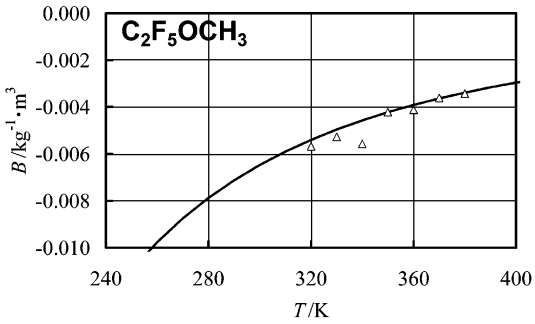

Figure 12. Temperature dependence of the second virial coefficient for $C_2F_5OCH_3$: △, experimental values by this work, vibrating-tube densimeter; - - -, calculated curve by eq 14.

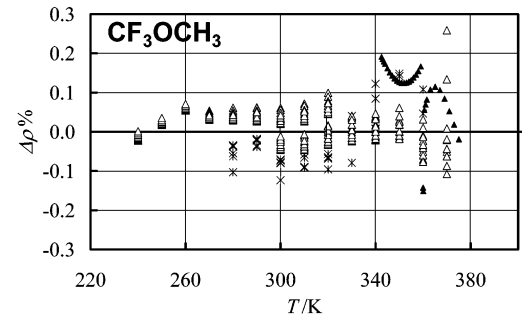

Figure 13. Relative density deviation of the liquid-phase *PVT* properties of CF_3OCH_3 from eq 17: △, this work, vibrating-tube densimeter; ∗, Morimoto;[3] ▲, Yoneda.[5]

Table 7. Numerical Constants for Eqs 17−20

	CF_3OCH_3	$C_2F_5OCH_3$
a_0	43.031 4	48.821 7
a_1	−73.801 4	−81.557 3
a_2	29.755 6	31.770 0
c_0	0.092 242	0.066 857
c_1	−0.141 198	−0.105 011
c_2	0.145 531	0.149 314
d_0	0.229 411	0.350 680
d_1	0.510 179	−0.071 879
d_2	−0.600 009	0.295 100
d_3	0.421 271	

to the present data obtained by the vibrating-tube densimeter apparatus. These are summarized in Table 7.

First, the density representation of the EoS thus developed was examined. Figures 13 and 14 illustrate the relative density deviation of the liquid density data reported for CF_3OCH_3 and $C_2F_5OCH_3$ from eq 17, respectively. Regarding the liquid density data for CF_3OCH_3, our data are well reproduced by eq 17 within ±0.1% except a few points at 370 K, that is 7.9 K below the critical

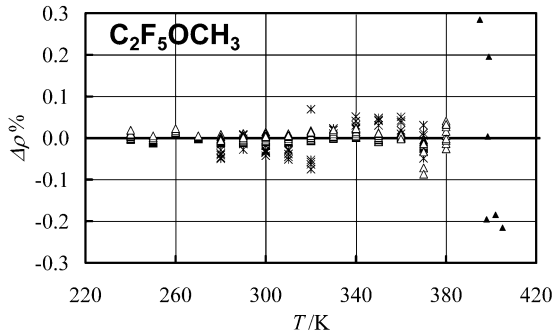

Figure 14. Relative density deviation of the liquid-phase *PVT* properties of $C_2F_5OCH_3$ from eq 17: △, this work, vibrating-tube densimeter; ∗, Ohta et al.;[4] ▲, Widiatmo et al.[6]

temperature (T_c = 377.921 K[1]). Those reported by Morimoto[3] also agree with the present EoS within ±0.15%, while the isochoric data by Yoneda[5] deviate by +0.2% in maximum.

As for $C_2F_5OCH_3$, all the present liquid density data have been confirmed to be reproduced by eq 17 excellently within ±0.04%. Those obtained by Ohta et al.[4] are also well represented within ±0.08%. By confirming satisfactory representation of the present data with a simple EoS, eq 17, it is suggested that our liquid density data obtained with the vibrating-tube densimeter apparatus have good continuity and reliability.

To discuss the soundness of the thermodynamic property surface of eq 17, we have derived other caloric properties from eq 17. To do that, we have estimated the isobaric heat capacities at the saturated-liquid state, c_p', by means of the corresponding state theory reported by Poling et al.,[20] which is given by

$$\frac{c_p' - c_p^0}{R} = 1.586 + \frac{0.49}{1 - T_r} + \omega\left[4.2775 + \frac{6.3(1 - T_r)^{1/3}}{T_r} + \frac{0.4355}{1 - T_r}\right] \quad (21)$$

where ω denotes the acentric factor and is defined by

$$\omega \equiv -\log\left(\frac{P_s}{P_c}\right)_{T_r=0.7} - 1.000 \quad (22)$$

We have calculated the acentric factors for CF_3OCH_3 and $C_2F_5OCH_3$ from eq 22 and the vapor pressure correlation, eq 10, which yields ω = 0.287 for CF_3OCH_3 and ω = 0.358 for $C_2F_5OCH_3$, respectively. Concerning the ideal gas isobaric heat capacity, c_p^0, for CF_3OCH_3 and $C_2F_5OCH_3$, there exist no experimental data or analytical studies reported. In the present study, therefore, it is calculated from the group-contribution prediction method proposed by Rihani and Draiswamy.[21] According to their method, the numerical parameters for the empirical c_p^0 correlation which is given in eq 23 are determined from the molecular structure of the fluid of interest. The estimated values of the constants c_1 through c_4 that were used in the present study for CF_3OCH_3 and $C_2F_5OCH_3$ are tabulated in Table 8.

$$c_p^\circ(T) = \sum_{i=0}^{3} c_i T^i \quad (23)$$

Then we have derived liquid-phase isobaric heat capacities for CF_3OCH_3 and $C_2F_5OCH_3$ by using the following thermodynamic relation

$$c_p = c_p' - \int_{P_s}^{P} T\left(\frac{\partial^2 v}{\partial T^2}\right)_P dP \quad (24)$$

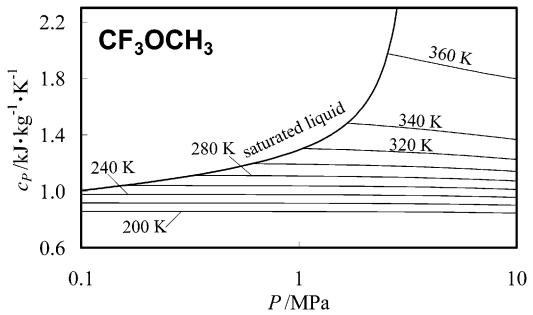

Figure 15. Liquid-phase isobaric heat capacity for CF_3OCH_3 calculated from eq 17: —, isotherms from 200 to 360 K; —, satulated-liquid.

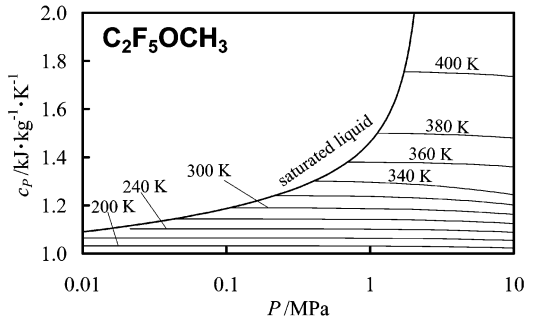

Figure 16. Liquid-phase isobaric heat capacity for $C_2F_5OCH_3$ calculated from eq 17: —, isotherms from 200 to 400 K; —, satulated-liquid.

Table 8. Numerical Constants in the c_p° Correlation, Eq 23

	CF_3OCH_3	$C_2F_5OCH_3$
c_0	1.9387	−1.0156
c_1/K^{-1}	7.6230×10^{-2}	1.2768×10^{-1}
c_2/K^{-2}	-4.9240×10^{-5}	-9.3440×10^{-5}
c_3/K^{-3}	1.0935×10^{-8}	2.3497×10^{-8}

Figures 15 and 16 show the pressure dependence of the calculated isotherms of the isobaric heat capacities in the liquid phase of CF_3OCH_3 and $C_2F_5OCH_3$, respectively. Since there exist no experimental heat capacity data for HFEs, we cannot compare these calculated isobaric heat capacities with experimental data. Our calculated isobaric heat capacities for CF_3OCH_3 and $C_2F_5OCH_3$ are confirmed to behave thermodynamically soundly even at higher temperatures. We have set the higher temperature limit of eq 17 to be $0.95T_c$, where the thermodynamic property surfaces according to eq 17 are certainly rational and physically sound. We have also examined behaviors of other derived properties including isothermal compressibilities, isochoric heat capacities, and speeds of sound for CF_3OCH_3 and $C_2F_5OCH_3$, and we confirmed again their thermodynamic soundness represented by eq 17.

Conclusions

Thermodynamic properties for a couple of pure hydrofluoroethers, CF_3OCH_3 and $C_2F_5OCH_3$, including *PVT* properties in both the gas phase and liquid phase, vapor pressures, and saturated-liquid densities, were obtained by means of the Burnett apparatus and the vibrating-tube densimeter apparatus. Our *PVT* data in the gas phase are

the first measurements concerning both HFE refrigerants. The liquid-phase *PVT* data were also obtained in the extended temperature range (240 to 380) K, at pressures up to 7 MPa, where no measured data were available up to the present. On the basis of the present measurements, we have developed a couple of equations of state (EoS's) such as the truncated virial EoS for the gas phase and a van der Waals type EoS for the liquid phase. By using these thermodynamic models, our measured data were well represented within satisfactory agreement. Thermodynamically sound behavior of the virial coefficients or heat capacities was also confirmed so that these thermodynamic models should establish a reasonable thermodynamic property surface. In addition to the present measurements, we have reported systematic information about thermodynamic properties of these important alternative refrigerants.

Literature Cited

(1) Yoshii, Y. Measurements of Saturation Densities and Critical Parameters for Alternative Refrigerants with Less Environmental Impact (in Japanese). M.S. Thesis, Keio University, Yokohama, Japan, 2001.

(2) Yoshii, Y.; Mizukawa, M.; Widiatmo, J. V.; Watanabe, K. Measurements of Saturation Densities in the Critical Region of Pentafluoroethy Methyl Ether (245cbE$\beta\gamma$). *J. Chem. Eng. Data* **2001**, *46*, 1050−1053.

(3) Morimoto, Y. A Study of Liquid-Phase Thermodynamic Properties for New Generation Refrigerants (in Japanese). M.S. Thesis, Keio University, Yokohama, Japan, 2001.

(4) Ohta, H.; Morimoto, Y.; Widiatmo, J. V.; Watanabe, K. Liquid-Phase Thermodynamic Properties of New Refrigerants: Pentafluoroethyl Methyl Ether and Heptafluoropropyl Methyl Ether. *J. Chem. Eng. Data* **2001**, *46*, 1020−1024.

(5) Yoneda, T. A Study of Thermodynamic Properties for New Refrigerant, CF_3OCH_3 (in Japanese). M.S. Thesis, Keio University, Yokohama, Japan, 2001.

(6) Widiatmo, J. V.; Tsuge, T.; Watanabe, K. Measurements of Vapor Pressures and *PVT* Properties of Pentafluoroethyl Methyl Ether and 1,1,1-Trifluoroethane. *J. Chem. Eng. Data* **2001**, *46*, 1442−1447.

(7) Widiatmo, J. V.; Watanabe, K. Studies on the New Generation Refrigerants: Fluorinated Ethers and Their Mixtures. *Proceedings of the 2002 JSRAE Annual Conference*, Okayama, Japan, November 2002, pp 519−522.

(8) Widiatmo, J. V.; Watanabe, K. Equations of State for Fluorinated Ether Refrigerants, CF_3OCH_3 and $(CF_3)_2CFOCH_3$. *Proc. of International Institute of Refrigeration (IIR/IIF), Commission B1* (CD-ROM), Paderborn, Germany, 2001; pp 71−78.

(9) Zhang, H.-L. Burnett Measurements and Thermodynamic Modeling for Several Hydrofluorocarbons and Their Binary Mixtures. Ph.D. Thesis, Keio University, Yokohama, Japan, 1996.

(10) *Guide to the Expression of Uncertainty in Measurement*; International Organization of Standardization (ISO): Switzerland, 1993; p 101.

(11) Kayukawa, Y.; Tada, S.; Zhang, H.-L.; Watanabe, K. Measurements of Gas-Phase *PVTx* Properties for the Ternary Mixtures Difluoromethane (1) + Pentafluoroethane (2) + 1,1,1-Trifluoroethane (3). *J. Chem. Eng. Data* **2002**, *47*, 1406−1410.

(12) Kayukawa, Y.; Watanabe, K. *P*ρ*Tx* Measurements for Gas-Phase Pentafluoroethane + Propane Mixtures by the Burnett Method. *J. Chem. Eng. Data* **2001**, *46*, 1025−1030.

(13) Kayukawa, Y.; Hasumoto, M.; Watanabe, K. Rapid Density-Measurement System with Vibrating Tube Densimeter. *Rev. Sci. Instrum.*, in press.

(14) Angus, S.; de Reuck, K. M.; Armstrong, B. *International Thermodynamic Tables of the Fluid State-6, Nitrogen*; Pergamon Press: Oxford, 1979. International Union of Pure and Applied Chemistry (IUPAC).

(15) Kul, I.; Des Marteau, D. D.; Beyerlein, A. L. Vapor-Liquid Equilibria of Novel Chemicals and Their Mixtures as R-22 Alternatives. *Fluid Phase Equilib.* **2000**, *173*, 263−276.

(16) Salvi-Narkhede, M.; Wang, B.-H.; Adcock, J. I.; Van Hook, W. A. Vapor pressures, Liquid Molar Volumes, Vapor Nonideality, and Critical Properties of Some Partially Fluorinated Ethers ($CF_3OCF_2CF_2H$, CF_3OCF_2H, and CF_3OCH_3), Some Perfluoroethers ($CF_3OCF_2OCF_3$, C.-$CF_2OCF_2OCF_2$, and C−$CF_2CF_2CF_2O$), and of CHF_2Br and CF_3CFHCF_3. *J. Chem. Thermdyn.* **1992**, *24*, 1065−1075.

(17) Wang, B.-H.; Adcock, J. L.; Mathur, S. B.; Van Hook, W. A. Vapor Pressures, Liquid Molar Volumes, Vapor Non-Idealities, and Critical Properties of Some Fluorinated Ethers: $CF_3OCF_2OCF_3$, $CF_3OCF_2CF_2H$, c-$CF_2CF_2CF_2O$, CF_3OCF_2H, and CF_3OCH_3 and of CCl_3F and CF_2ClH. *J. Chem. Thermodyn.* **1991**, *23*, 699−710.

(18) Yasumoto, M. Research Institute of Innovative Technology for the Earth (RITE), private communication, 1999.

(19) Sato, H. A study on Thermodynamic Property Surface of Water and Steam under High Pressures (in Japanese). Ph.D. Thesis, Keio University, Yokohama, Japan, 1981.

(20) Poling, B. E.; Prausnitz, J. M.; O'Connell, J. P. *The Properties of Gases and Liquids*, 5th ed.; McGraw-Hill: New York, 2000.

(21) Rihani, D. N.; Doraiswamy, L. K. Estimation of Heat Capacity of Organic Compounds from Group Contributions. *Ind. Eng. Chem. Fundam.* **1965**, *4*, 17−21.

Received for review December 16, 2002. Accepted June 3, 2003.

JE025657+